Observations of Isotopic Heterogeneities Toward Embedded Cores and Binary Systems: Potential Tracers of Varying Chemical Evolutionary Pathways in Protostellar Gas

Rachel L. Smith[1,2], Klaus M. Pontoppidan[3], Geoffrey A. Blake[4,5], A. C. Adwin Boogert[6], Alexandra C. Lockwood[4]

[1]North Carolina Museum of Natural Sciences, 121 West Jones Street, Raleigh, North Carolina, 27603 (rachel.smith@naturalsciences.org),[2]Appalachian State University, Department of Physics & Astronomy, Boone, North Carolina, 28608, [3]Space Telescope Science Institute, Baltimore, MD, [4]California Institute of Technology, Division of Geological and Planetary Sciences, [5]Division of Chemistry and Chemical Engineering, Pasadena, CA, [6]IPAC, NASA Herschel Science Center, California Institute of Technology, Pasadena, CA

SUMMARY

Using the CRIRES (Very Large Telescope) spectrograph at very high resolution ($R \sim 95{,}000$), CO isotopologues ($^{12}C^{16}O$, $^{13}C^{16}O$, $^{12}C^{18}O$, $^{12}C^{17}O$) were observed along 14 lines-of-sight toward embedded protostars, disks, and foreground clouds, representing 7 local star-forming regions. Abundance ratios of [^{12}CO]/[^{13}CO] ranged from ~ 85 to 165, with several values significantly higher than the solar system (~ 87 [1]) and local Interstellar Medium (ISM) (~ 68 [2]). The [^{12}CO]/[^{13}CO] for each of the components of the binary disk systems, DoAr24E (Ophiuchus) [98 ± 1 and 102 ± 3] and EC90 (Serpens) [130 ± 4 and 140 ± 16] were found to be within error of each other. The low-temperature ratio for the northern component of the V V CrA (N; Corona Australis) binary is [127 ± 2], the same value obtained for its southern, cold-gas companion, V V CrA (S) [127 ± 1]. A weak but suggested trend was found between total CO ice abundance and [^{12}CO]/[^{13}CO] in the gas, suggesting that interplay between the CO ice and gas-phase reservoirs may be a partial explanation for the heterogeneity in [^{12}CO]/[^{13}CO]. Heterogeneity was found in [^{16}O]/[^{18}O] and [^{16}O]/[^{17}O] toward 8 targets. Excesses of ^{16}O along a mass-independent line are found in warm gas for the disks, V V CrA (N); $^{16}O/^{18}O = 740 \pm 15$; $^{16}O/^{17}O = 3080 \pm 440$) and HL Tau ($^{16}O/^{18}O = 790 \pm 80$; $^{16}O/^{17}O = 3500 \pm 660$), lending support for CO self-shielding in disks as an explanation for the oxygen isotope anomaly in the solar system [2,3].

These data thus far suggest that isotopic heterogeneity in [^{12}CO]/[^{13}CO] could be tracing varying chemical pathways in embedded cores in different clouds, and in cores dispersed within the same cloud, as compared to isotopic homogeneity observed in the binary systems (gas within ~ 200 to 400 AU). Further, these results oppose Galactic Chemical Evolution model implications that solar nebula analogues should be isotopically similar to their parent clouds [4,5; *Smith, Pontoppidan, Young, Morris, submitted*]. New data from Keck-NIRSPEC ($R \sim 25{,}000$) expand our targets to include massive young stellar objects in high-UV fields at a range of Galactocentric radii (R_{GC}).

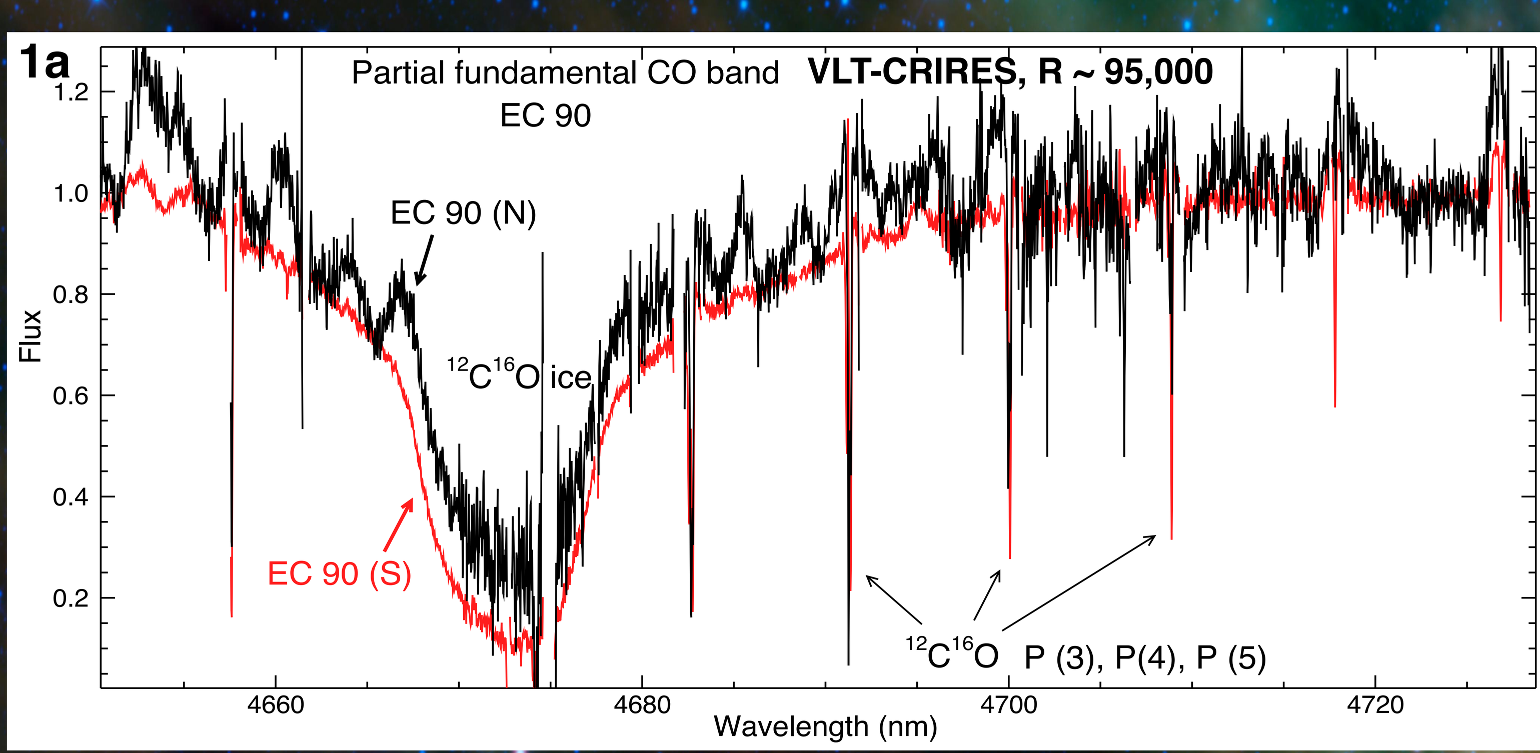

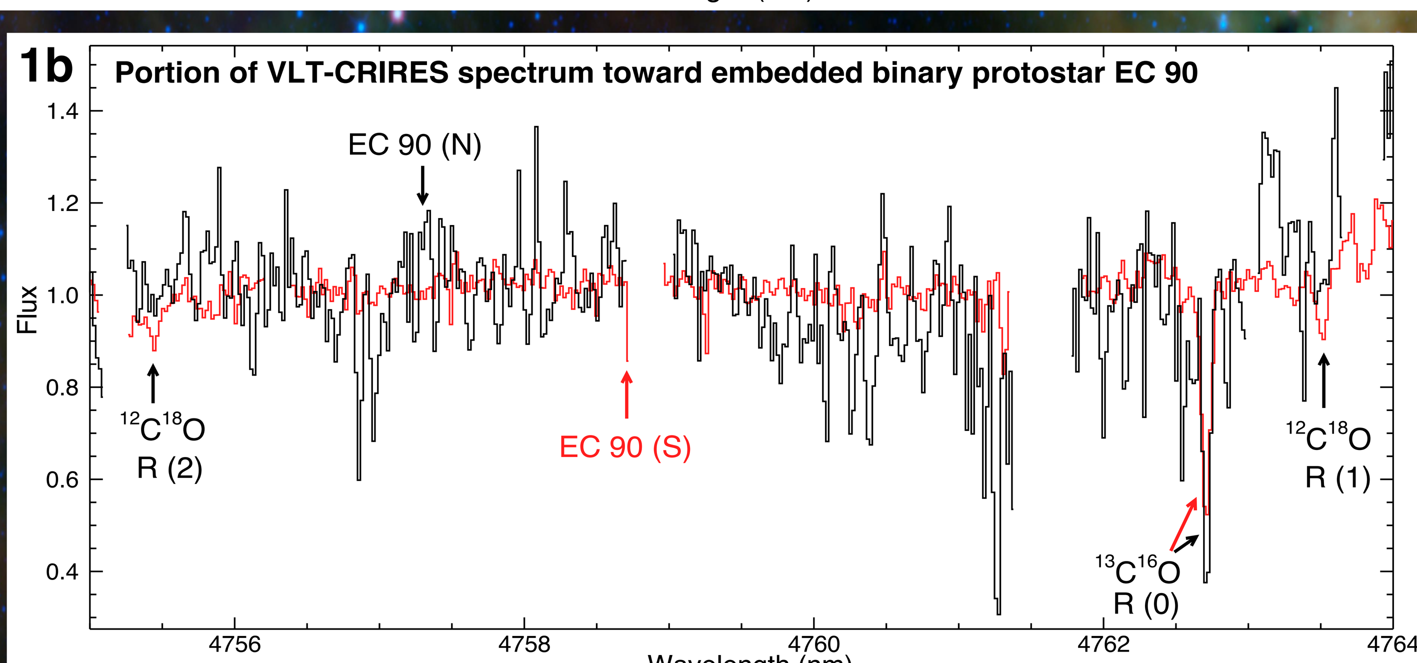

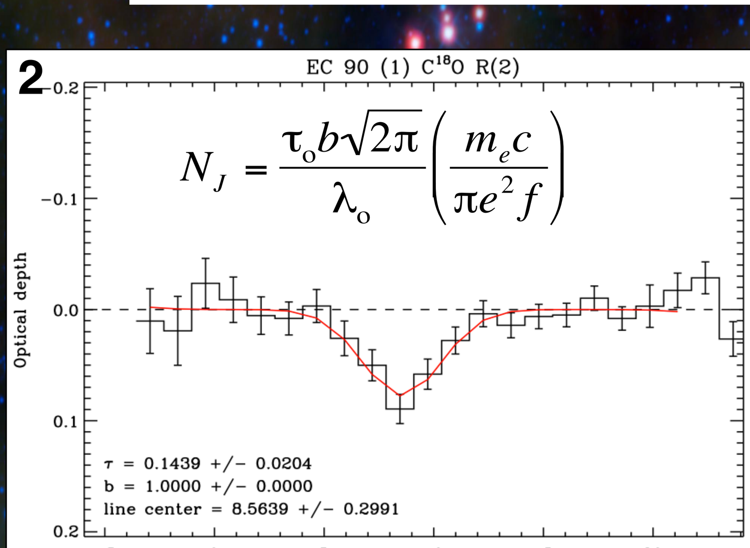

OBSERVATIONS and METHODS

Fig. 1a (top, left): CRIRES CO rovibrational (υ = 1 - 0) spectra for the binary, EC 90 (N,S). Selected CO isotopologue lines are marked. **Fig. 1b** (above): zoom of the (υ = 1 - 0) spectra showing several specific rovibrational lines.

Fig. 2 (left): Gaussian fit to the EC 90 (S) $^{12}C^{18}O$ R(2) spectral line convolved with the CRIRES broadening (~ 3.2 km/s). Each CRIRES line in this study was so modeled to obtain optical depth (τ) and intrinsic line width (b), which were used to compute each line column density (N_J).

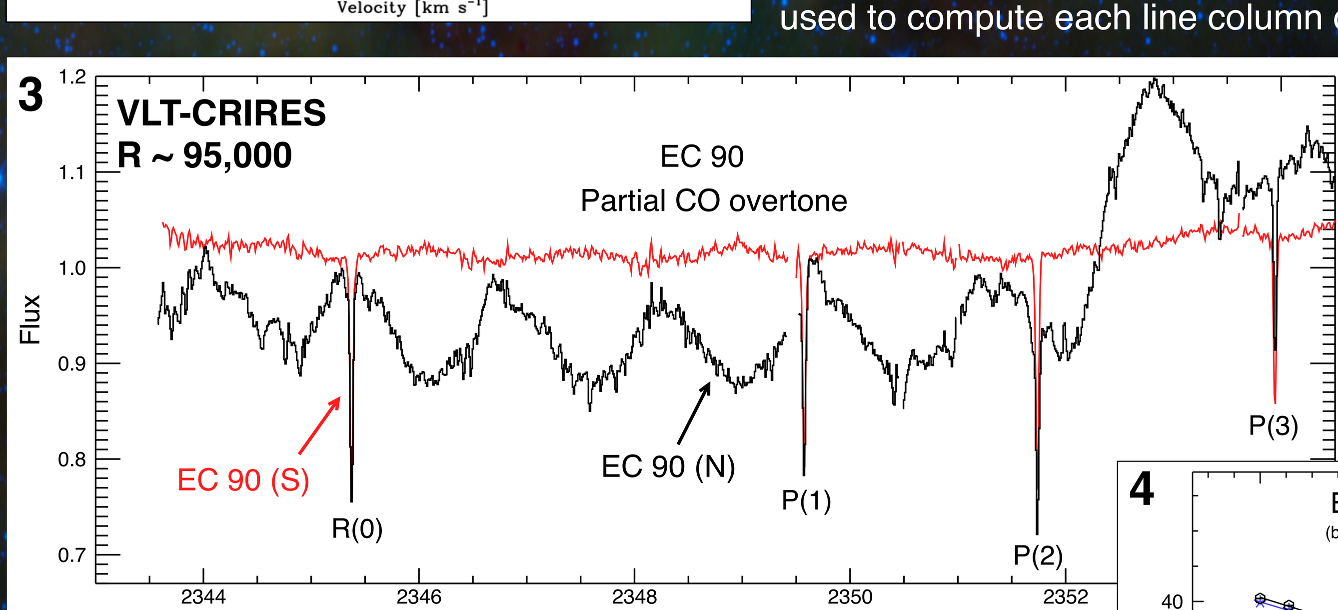

Fig 3 (left): portion of the overtone (υ = 2 - 0), ~100 times weaker than the fundamental. All $^{12}C^{16}O$ column densities were derived from the overtone bands in order to offset significant saturation issues in (υ = 1 - 0).

Figs. 4 (right): sample rotational diagram from this study, here showing results for the two EC 90 lines-of-sight. Each point represents an observed rovibrational line. Total column densities were calculated by summing the measured column densities and assuming a Boltzmann distribution for the remaining lines. Either a single-temperature (e.g. EC 90 and other objects where *only* cold gas was observed) or two-temperature model (warm *and* cold gas observed) was assumed for all objects in the study.

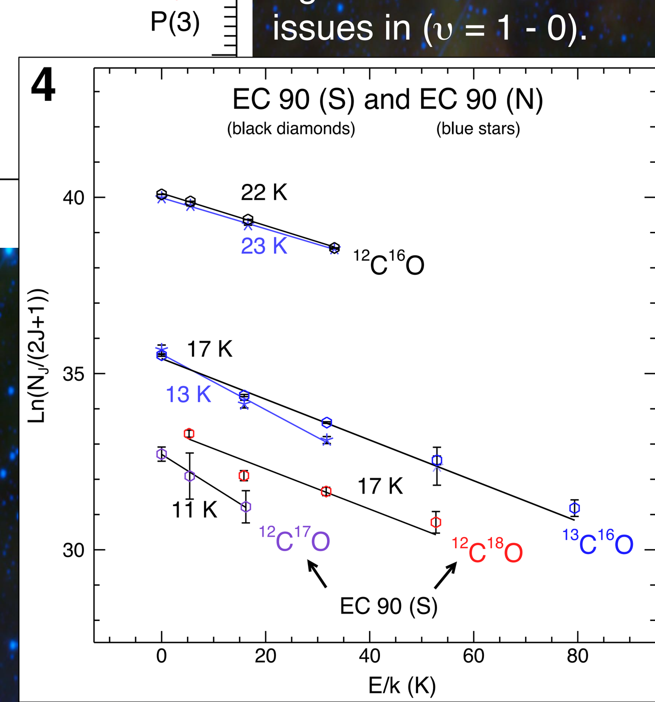

RESULTS and DISCUSSION

Fig. 5 (below, left): the [^{12}CO]/[^{13}CO] abundance ratios (~ 85 to 165) in our latest CRIRES sample in relation to the local ISM, solar system, and data from the literature [1,2,6-12] plotted vs. Galactocentric radius (R_{GC}). Significant heterogeneity (values ranging from ~ 85 to 165) was observed in the embedded cores in the same cloud (Ophiuchus) and in cores in different clouds, as compared to the binary systems (colored arrows).

Fig. 6 (below, right): heterogeneity in the oxygen isotope data observed between parent clouds, as well as in the V V CrA binary (although results for V V CrA (S) are based on only the few $^{12}C^{18}O$ and $^{12}C^{17}O$ lines observed toward this component). Signatures for isotope-specific photodissociation in oxygen were observed in V V CrA (N) and HL Tau, [6, 13, 14; *Smith, Pontoppidan, Young, Morris, submitted; new data*].

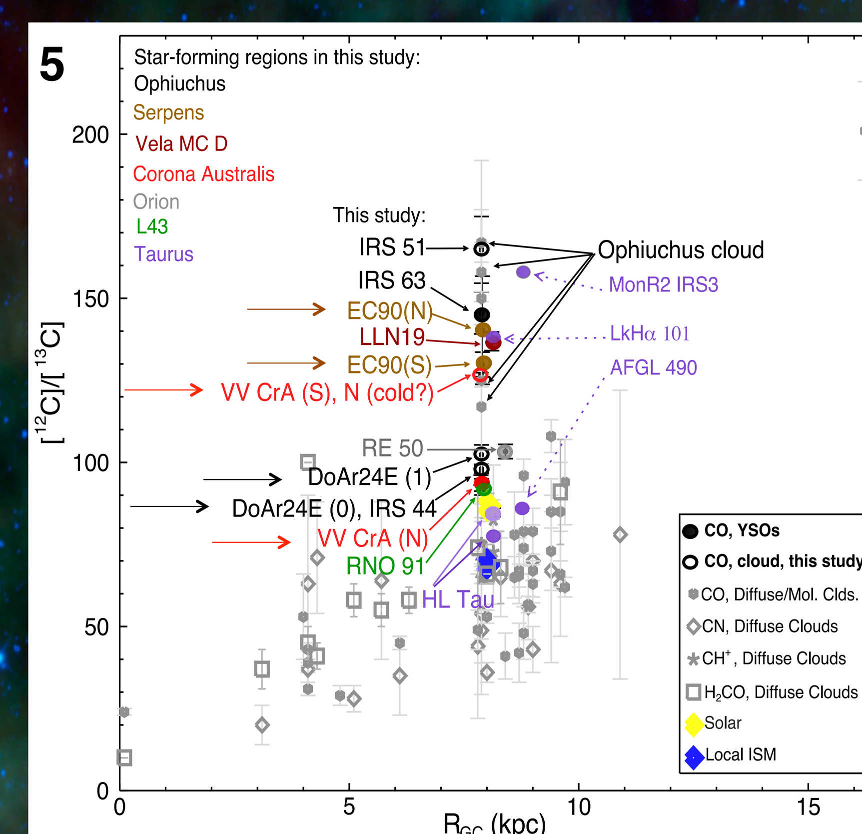

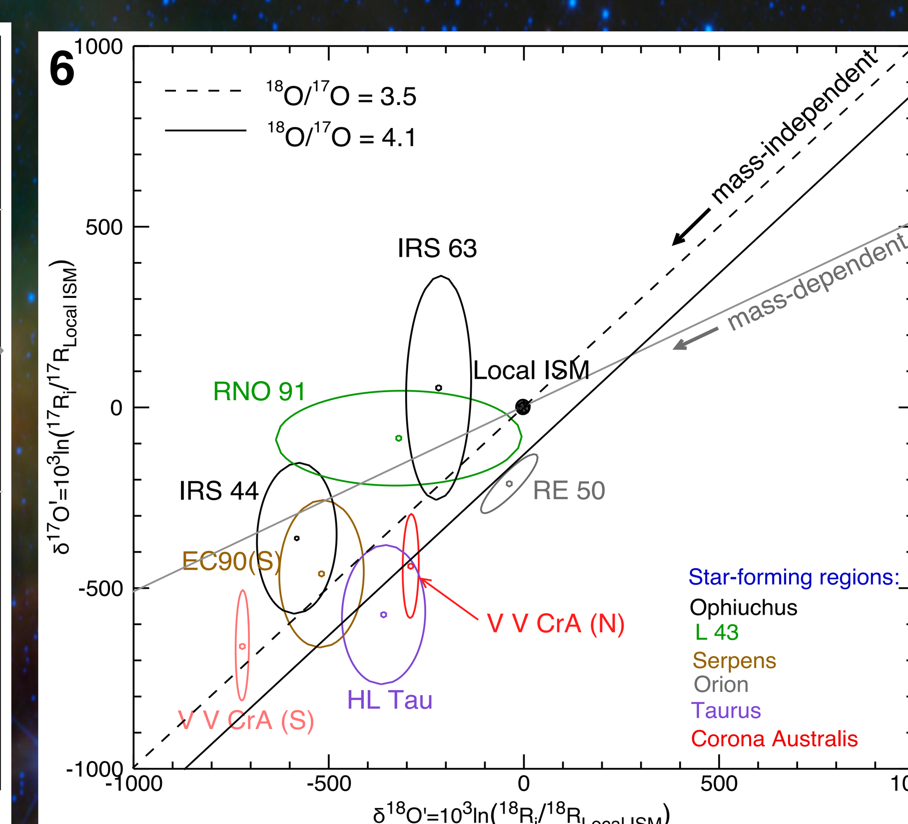

Fig. 7a (below): relation between the total CO ice abundance (derived using optical depths from [15,16]) and [^{12}CO]/[^{13}CO] gas-phase abundance ratios. A potential weak trend suggests that interaction between the ice and gas reservoirs could be a partial explanation for the [^{12}CO]/[^{13}CO] heterogeneity in the gas.

Fig. 7b (below): as in **7a**, showing only those objects where cold gas *only* was observed; these sources may be the most reliable indicators of gas-ice interactions because 1) cold gas should interact more directly with the ice than the warm gas, and 2) cold-gas ratios are the most robust when derived from single-temperature fit to the lines [Figs 7a and 7b: 14; *Smith et al., submitted; new data*].

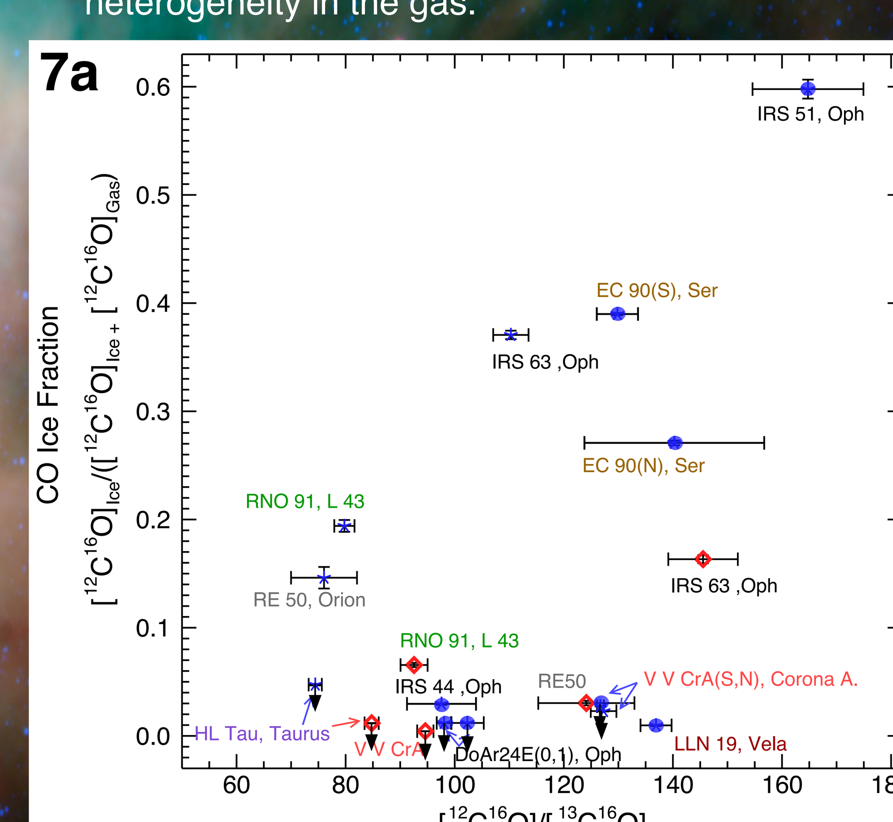

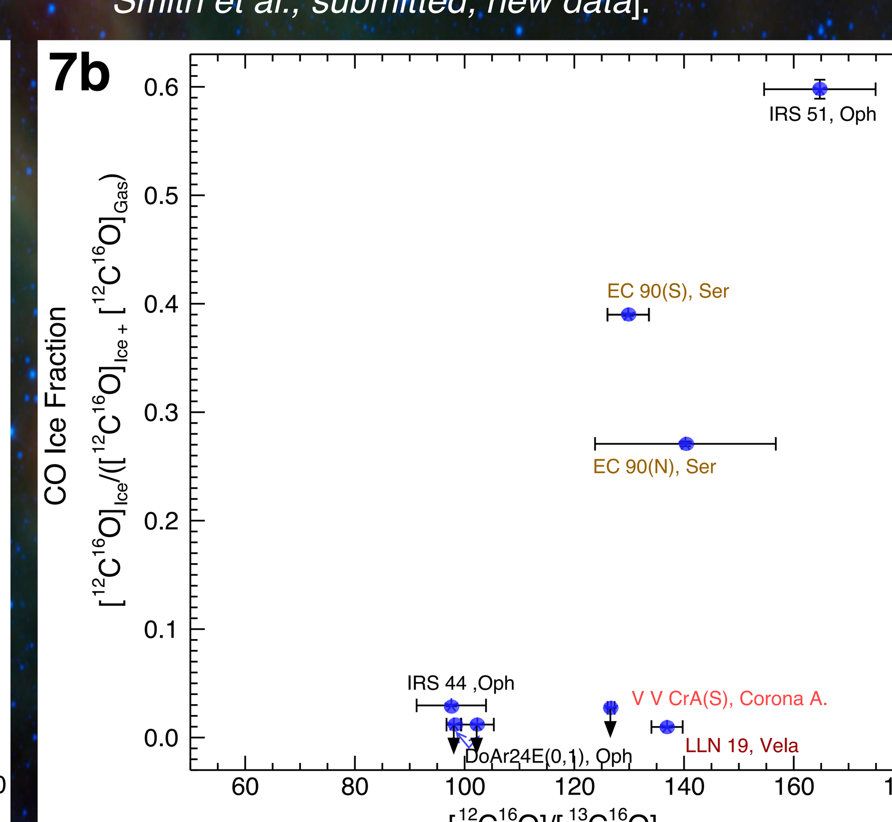

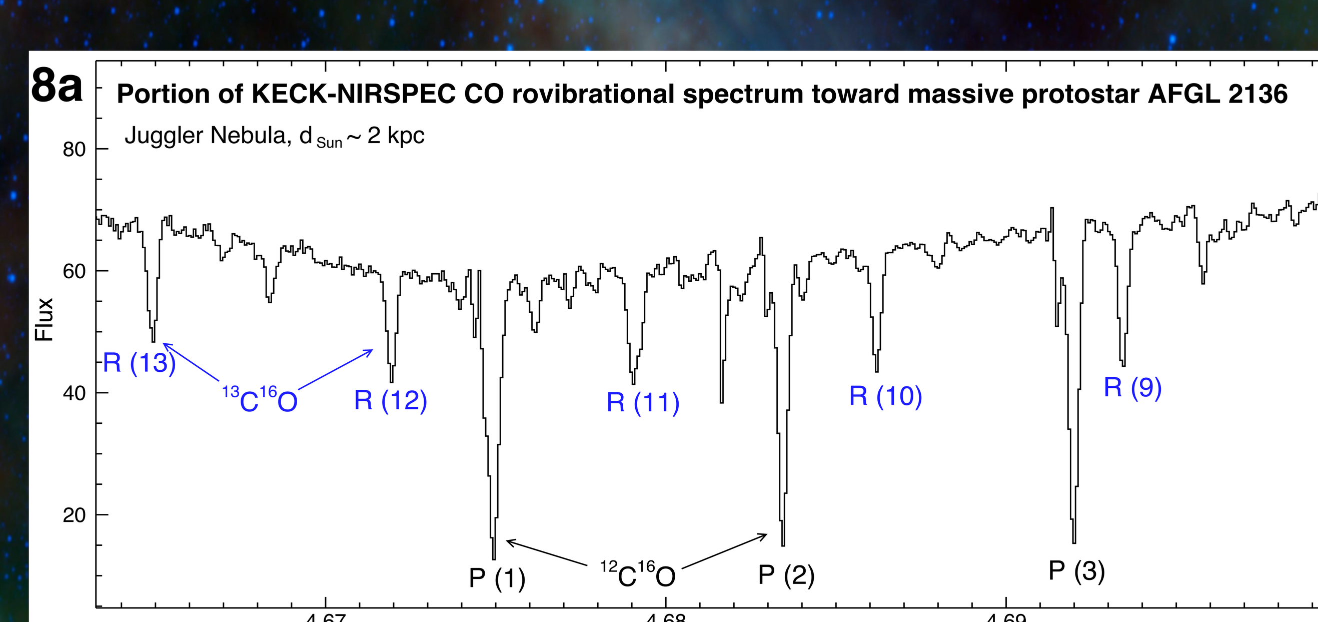

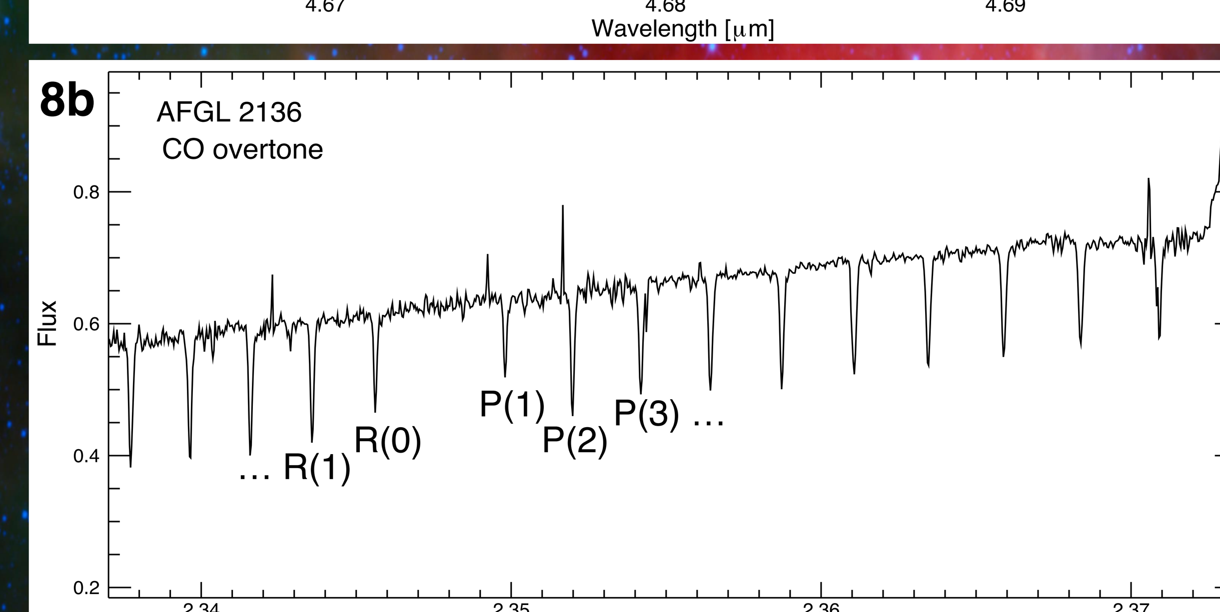

MASSIVE PROTOSTARS

New CO near-infrared data of massive protostars along the Galactic plane were obtained with Keck-NIRSPEC ($R \sim 12$ km/s), expanding our current data set of precise CO gas-phase isotopologues to include young stellar objects spanning a range of R_{GC}, high-UV fields and CO ice abundance along the lines-of-sight. Sample spectra for AFGL 2136 are shown in **Figs 8a** (top left) and **8b** (bottom left).

CONCLUSIONS: Significant [^{12}CO]/[^{13}CO] heterogeneity observed in embedded protostars and young stellar objects could be tracing varying chemical paths for protostellar cores separated in the parent cloud. Results also indicate greater [^{12}CO]/[^{13}CO] homogeneity within ~200 to 400 AU for low-mass protostars. A suggested trend in the data lends support for ice-gas interaction influencing gas-phase [^{12}CO]/[^{13}CO]. For the oxygen isotopes, heterogeneity may correlate with protostellar evolutionary stage. This ongoing study now includes new gas-phase observations of massive protostars and analysis of additional isotopic reservoirs [17,18]. Future observations will include additional cold protostellar regions to further study of ice-gas interactions.

Image: *WISE* image of the *Rho Ophiuchi star-forming cloud*. Credit: NASA/JPL-Caltech/UCLA

References: [1] Scott P.C. et al. (2006) A&A. 456, 675-688. [2] Milam S.N. et al. (2005) ApJ 634, 1126-1132. [3] Clayton R.N. et al. (1973) *Science 182*, 458-488. [4] Lyons J.R. and Young E.D. (2005) *Nature 435, 7040*, 317- 320. [5] Prantzos N. et al. (1996) *A&A 309*, 760-774. [6] Smith R.L. et al. (2009) ApJ 701, 163-175. [7] Brittain S.D. et al. (2005) ApJ 626, 283-291. [8] Langer W.D. and Penzias A.A. (1993) ApJ 408, 539-547. [9] Bensch et al. (2001) ApJ 562, L185-L188. [10] Goto M. et al. (2003) ApJ 598, 1038-1047. [11] Federman S.R. et al. (2003) ApJ 591, 989-999.[12] Lambert D.L. et al. (1994) ApJ 420, 756-771. [13] Smith R.L. et al. (2011) 42nd LPI, 1608, 1281. [14] Smith R. L. et al. (2013) 44th LPI, #2698. [15] Pontoppidan K.M. et al. (2003) A&A 408, 981-1007. [16] Thi W.-F. et al. (2006) A&A 449, 251-265. [17] Boogert A.C.A. et al. (2000) A&A 353, 349-362. [18] Boogert A.C.A. et al. (2002) ApJ 577, 271-280